

Electronic supplementary information (ESI) for:

Semi-Transparent Quaternary Oxynitride Photoanodes on GaN Underlayers

Zili Ma,^{a,b} Karolina Piętak,^{c,d} Jędrzej Piątek,^b Justin Reed DeMoulied,^e Anna Rokicinska,^f Piotr Kuśtrowski,^f Richard Dronskowski,^{a,g} Sebastian Zlotnik,^{c,h} Robert H. Coridan,^{e*} and Adam Slabon^{b*}

^a Institute of Inorganic Chemistry, RWTH Aachen University, 52056 Aachen, Germany.

^b Department of Materials and Environmental Chemistry, Stockholm University, 10691 Stockholm, Sweden

^c Łukasiewicz Research Network, Institute of Electronic Materials Technology, Wolczyńska 133, 01-919 Warsaw, Poland

^d Warsaw University of Technology, Faculty of Chemistry, Noakowskiego 3, 00-664 Warsaw, Poland

^e Department of Chemistry and Biochemistry, University of Arkansas, Fayetteville, Arkansas 72701, United States

^f Faculty of Chemistry, Jagiellonian University, Gronostajowa 2, 30-387 Krakow, Poland

^g Hoffmann Institute of Advanced Materials, Shenzhen Polytechnic, 7098 Liuxian Boulevard, Nanshan District, Shenzhen, China

^h Institute of Applied Physics, Military University of Technology, 2 Kaliskiego Str., 00-908 Warsaw, Poland

* Corresponding authors e-mail: adam.slabon@mmk.su.se; rcoridan@uark.edu

Table of Contents:

I. Experimental Methods

- 1.1 Preparation of sapphire (Al₂O₃)/GaN substrate
- 1.2 Fabrication of LaTiO₂N thin film on Al₂O₃/GaN
- 1.3 Fabrication of SrTaO₂N thin film on Al₂O₃/GaN
- 1.4 Atomic Layer Deposition of Ta₂O₅
- 1.5 Characterization
- 1.6 Photoelectrochemical measurements

II. Supplemental Figures

Fig. S1 Schematic illustration of a wireless artificial leaf tandem cell configuration for overall water splitting.

Fig. S2 XPS spectrum of TaO_xN_y film on Al₂O₃/GaN substrate in the Ta 4f region.

Fig. S3 SEM micrograph of TaO_xN_y film on Al₂O₃/GaN substrate.

Fig. S4 SEM micrograph at low magnification of Al₂O₃/GaN/TaO_xN_y.

Fig. S5 Chronoamperometry curve of TaO_xN_y film measured at 1.23 V versus RHE in 0.1 M NaOH under chopped AM 1.5G solar simulated light (100 mW cm⁻²).

Fig. S6 SEM micrograph at low magnification of LaTiO₂N film on Al₂O₃/GaN substrate.

Fig. S7 Cross-sectional SEM image of the LaTiO₂N film on Al₂O₃/GaN substrate.

Fig. S8 SEM micrograph of SrTaO₂N film on Al₂O₃/GaN substrate.

Fig. S9 Enlarged view of the data from Fig. 4d of the main manuscript.

III. References

I. Experimental Methods

1.1 Preparation of sapphire (Al_2O_3)/GaN substrate

2 μm -thick gallium nitride (GaN) epitaxial structure was grown on 2-inch double side polished Al_2O_3 (sapphire) substrate, with maximum cut-off 0.25° . The growth was conducted in low pressure metalorganic vapor phase epitaxy reactor (LP MOVPE) – AIX 200/4 RF-S, employing the consecutive precursors: trimethylaluminum (TMAI), trimethylgallium (TMGa) and ammonia (NH_3), while hydrogen (H_2) and nitrogen (N_2) were used as the carrier gases. In the MOVPE system a temperature was in situ controlled by emissivity corrected pyrometry using a Laytec EpiCurve TT system. The epitaxy process was conducted at approximately 1373 K and 200 mbar. After the process, the GaN/ Al_2O_3 structure was cut into 10×15 mm sample pieces.

1.2 Fabrication of LaTiO_2N thin film on Al_2O_3 /GaN

A modified method for $\text{La}_2\text{Ti}_2\text{O}_7$ thin film preparation was employed to make the precursor solution.¹⁻³ Briefly, 5 ml of 2-methoxyethanol (99.8%, Sigma-Aldrich), 4 ml of acetic acid (99.9+%, Alfa Aesar) and 1 ml of acetylacetone (99%, Merck) were mixed together by stirring. 1.0825 g of $\text{La}(\text{NO}_3)_3 \cdot 6\text{H}_2\text{O}$ (99.9%, Alfa Aesar) was dissolved into above solution and the mixture was stirred for 1 h. Afterward, 0.8509 g of titanium(IV) butoxide (97%, Sigma-Aldrich) was added dropwise under strong stirring, the mixture was stirred for additional 3 h to get clear solution containing ~ 0.25 M of La and Ti in molar ratio of 1:1. The solution was used to fabricate films by spin coating at 3000 rpm for 20 s on Al_2O_3 /GaN substrate in air, the film was dried on a hot plate of 573 K for ~ 5 min to remove organic constituents. Afterwards, the substrate was calcinated at 773 K for 1 h to decompose all organic components forming oxide. The oxide was converted to LaTiO_2N oxynitride by nitridation under flows of NH_3 (15 mL min^{-1}) and H_2 (5 mL min^{-1}) at 1148 K for 2 h at a ramping rate of 10 K min^{-1} .

1.3 Fabrication of SrTaO_2N thin film on Al_2O_3 /GaN

The precursor solution was prepared by using a modified process for Sr-Ta-O perovskite thin film.⁴ Inert atmosphere was used to handle the compounds for solution preparation. In short, 0.304 g of $\text{Ta}(\text{OCH}_2\text{CH}_3)_5$ (99.95%, Alfa Aesar) was added dropwise to 0.154 g of $\text{Sr}(\text{O}_2\text{CCH}_3)_2$ (Sigma-Aldrich), then 3.0 mL of acetic acid (99.9+%, Alfa Aesar) was added to the above mixture. The slurry was stirred for 1 h to obtain a clear solution containing ~ 0.25 M of Sr and Ta in molar ratio of 1:1. It should be noted that the solution should be freshly synthesized before each use. The solution was used to fabricate films by spin coating at 3000 rpm for 20 s on Al_2O_3 /GaN substrate in air, the film was dried on a hot plate of 573 K for ~ 5 min to remove organic constituents. Afterwards, the substrate was calcinated at 773 K for 1 h to decompose all organic components forming oxide. The oxide was converted to SrTaO_2N oxynitride by nitridation under flows of NH_3 (15 mL min^{-1}) and H_2 (5 mL min^{-1}) at 1148 K for 2 h at a ramping rate of 10 K min^{-1} .

1.4 Atomic Layer Deposition of Ta_2O_5

Tantalum pentoxide thin films were synthesized via atomic layer deposition (GEMStar XT; Arradiance, Inc.) using pentakis(dimethylamino)tantalum(V) (PDMAT, 99.99%; Sigma-Aldrich) and H_2O (HPLC grade; VWR Analytical) as precursors. Ultra-high-purity N_2 (99.999%, Airgas) was used as the carrier gas in the reactor and was controlled by an automated mass flow controller (20 sccm) for the entire deposition. The sample substrates were placed in the chamber held at 423 K, while the PDMAT precursor cylinder was heated to 379 K for the duration of deposition. Each cycle of the deposition consisted of a 100 ms precursor pulse of PDMAT, a chamber purge of 15s, a 15 ms H_2O pulse, and a second purge of 25s. This sequence was repeated a total of 600 times. This procedure resulted in a Ta_2O_5 film of roughly 20 nm (by cross-sectional scanning electron microscopy) for films grown for calibration on a silicon wafer coated with a thermally-grown oxide layer.

1.5 Characterization

X-ray diffraction (XRD) patterns were recorded with a Panalytical X'Pert Pro system configuration with $\text{Cu K}\alpha$ radiation at grazing incidence mode to minimize the contribution related to the substrate.

Surface morphology was characterized using a scanning electron microscope (SEM, JSM-7000F, JEOL) at accelerating voltage of 15 kV.

Ultraviolet-visible (UV-vis) transmittance spectra were collected by using UV-2600 (Shimadzu) spectrometer in the wavelength range of 300-900 nm.

Chemical surface composition was determined by X-ray photoelectron spectroscopy (XPS) using a monochromatized aluminum source $\text{Al K}\alpha$ ($E = 1486.6 \text{ eV}$) and a hemispherical VG SCIENTA R3000 analyzer. An adventitious C 1s feature at 284.6 eV was used to calibrate the measured spectrum.

1.6 Photoelectrochemical measurements

Photoelectrochemical (PEC) measurements were carried out in a three-electrode PEC cell (WAT Venture) with a potentiostat (PalmSens4, PalmSens BV) in 0.1 M NaOH aqueous solution (pH 13) under AM 1.5G simulated sunlight. The AM 1.5G simulated solar illumination was generated by a solar light simulator (class-AAA 94023A, Newport) with an ozone-free 450 W xenon short-arc lamp. The as-prepared film on the Al_2O_3 /GaN substrate, a 1 M Ag/AgCl electrode, and a platinum wire were used as the working, reference, and counter electrodes, respectively. The measured potentials versus 1 M Ag/AgCl have been converted to the reversible

hydrogen electrode (RHE) scale according to the Nernst equation ($E_{\text{RHE}} = E_{\text{Ag/AgCl}}^0 + 0.059 \times \text{pH} + E_{\text{Ag/AgCl}}$). Linear sweep voltammetry (LSV) curves were performed at a scan rate of 10 mV s^{-1} under chopped illumination. Chronoamperometry curves were recorded at a constant bias 1.23 versus RHE under chopped illumination.

II. Supplemental Figures

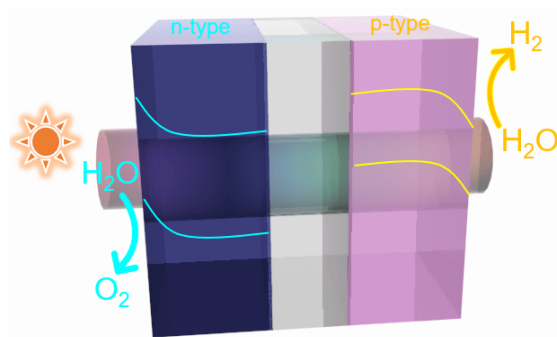


Fig. S1 Schematic illustration of a wireless artificial leaf tandem cell configuration for overall water splitting. The n-type and p-type semiconducting photoelectrodes are serially connected with a transparent conductive layer.

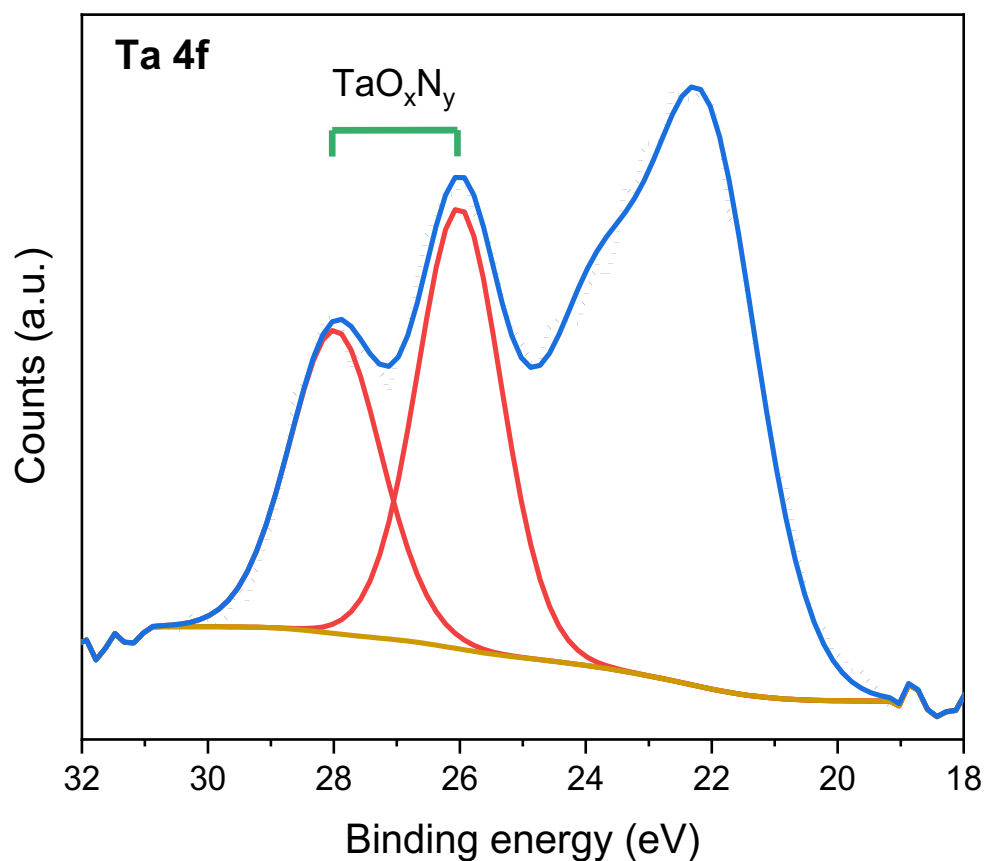


Fig. S2 XPS spectrum of TaO_xN_y film on $\text{Al}_2\text{O}_3/\text{GaN}$ substrate in the Ta 4f region.

As shown in Fig. S2, the fragment of the XPS spectrum in the range of binding energy between 20 eV and 30 eV is quite rich in photoemission from different electron levels. Below 24.8 eV, the overlapped XPS O 2s and Ga 3d peaks are observed. However, at higher binding energy the clear doublet of the Ta $4f_{7/2}$ and Ta $4f_{5/2}$ peaks is distinguished at 26.0 eV and 28.0 eV, respectively. Such positions of these peaks confirm that Ta exists rather in the N-doped Ta_2O_5 phase than Ta_3N_5 on the outermost surface.⁵

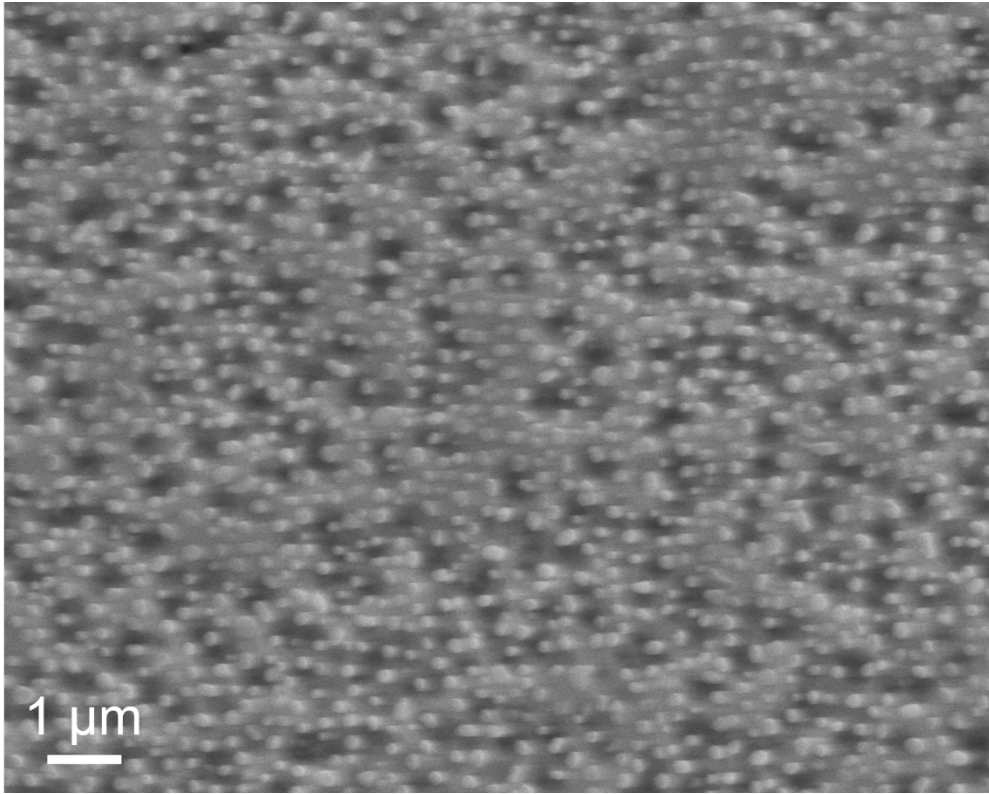


Fig. S3 SEM micrograph of TaO_xN_y film on Al₂O₃/GaN substrate.

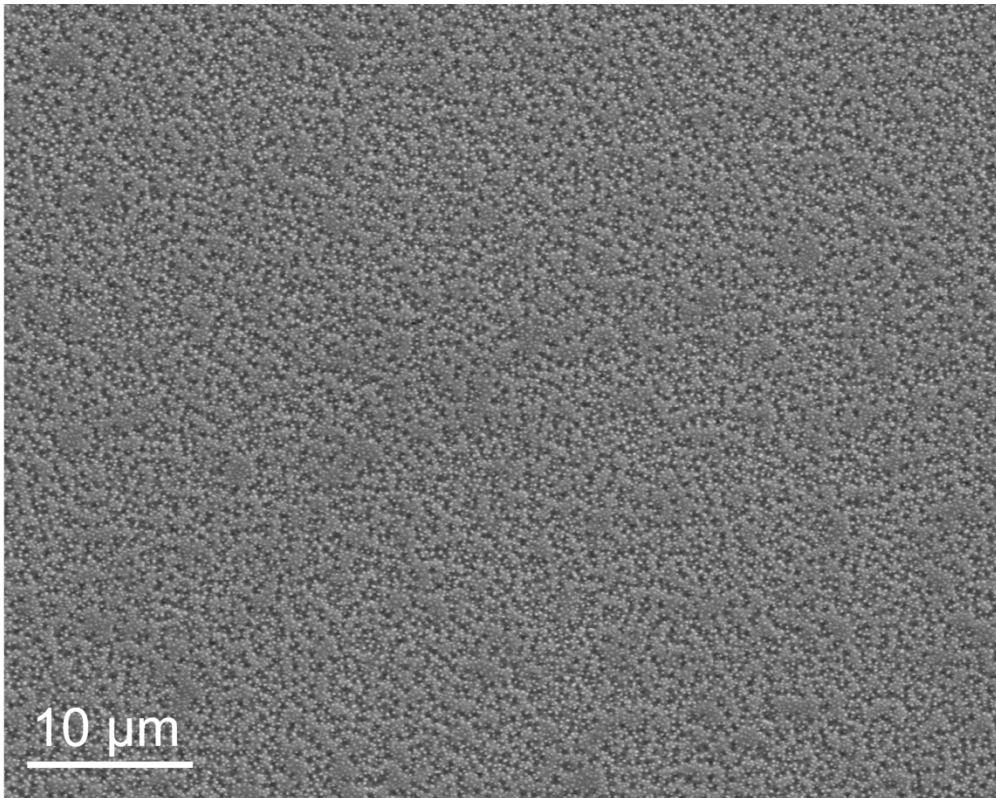


Fig. S4 SEM micrograph at low magnification of Al₂O₃/GaN/TaO_xN_y.

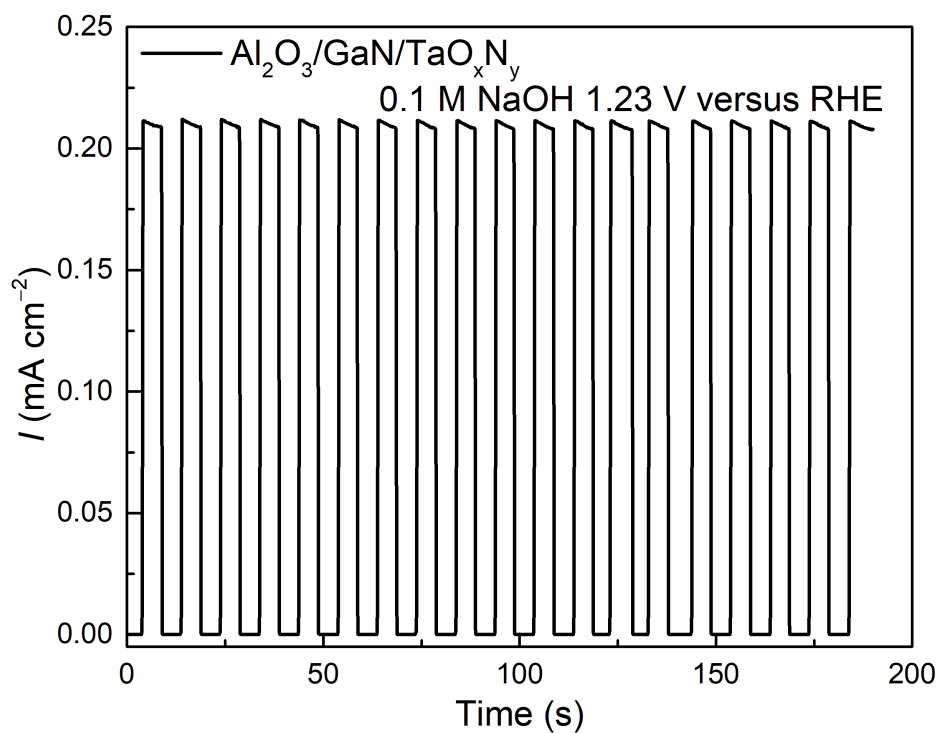


Fig. S5 Chronoamperometry curve of TaO_xN_y film measured at 1.23 V versus RHE in 0.1 M NaOH under chopped AM 1.5G solar simulated light (100 mW cm^{-2}).

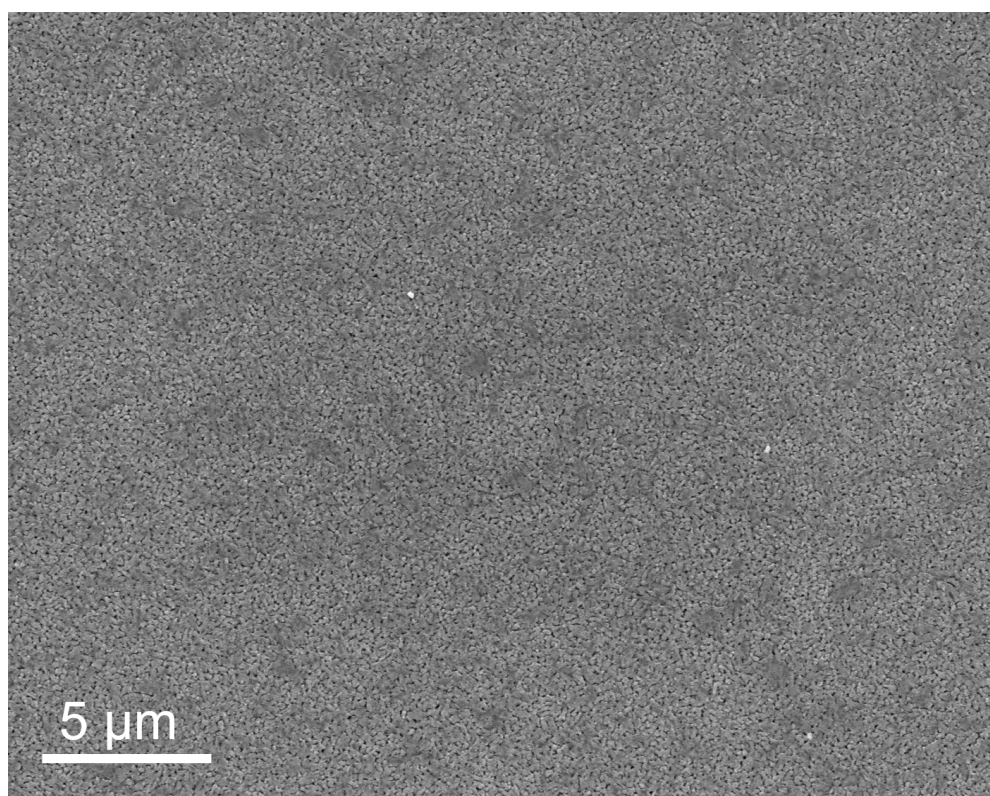


Fig. S6 SEM micrograph at low magnification of LaTiO_2N film on $\text{Al}_2\text{O}_3/\text{GaN}$ substrate.

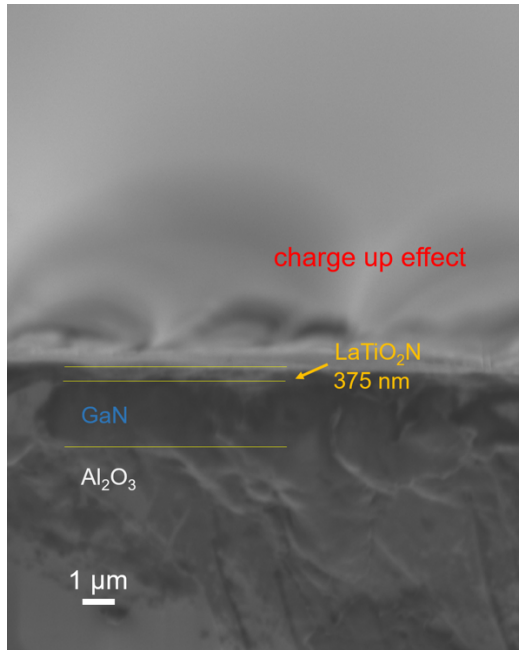


Fig. S7 Cross-sectional SEM image of the LaTiO₂N film on Al₂O₃/GaN substrate.

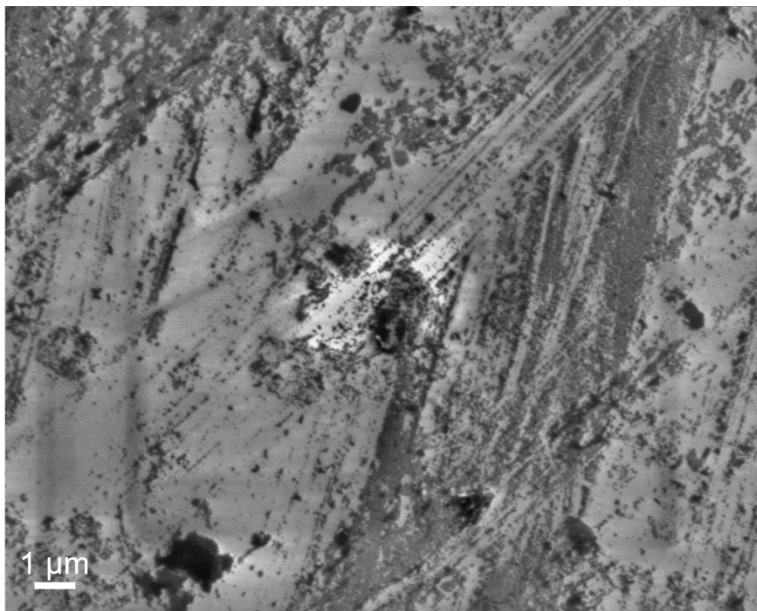


Fig. S8 SEM micrograph of SrTaO₂N film on Al₂O₃/GaN substrate.

The morphology of SrTaO₂N film looks smooth with some defects, very similar to its oxide precursor film.⁴ Comparing to the LaTiO₂N film, one can realize that the precursor solution has prominent effect on the morphology of deposited films via spin-coating.

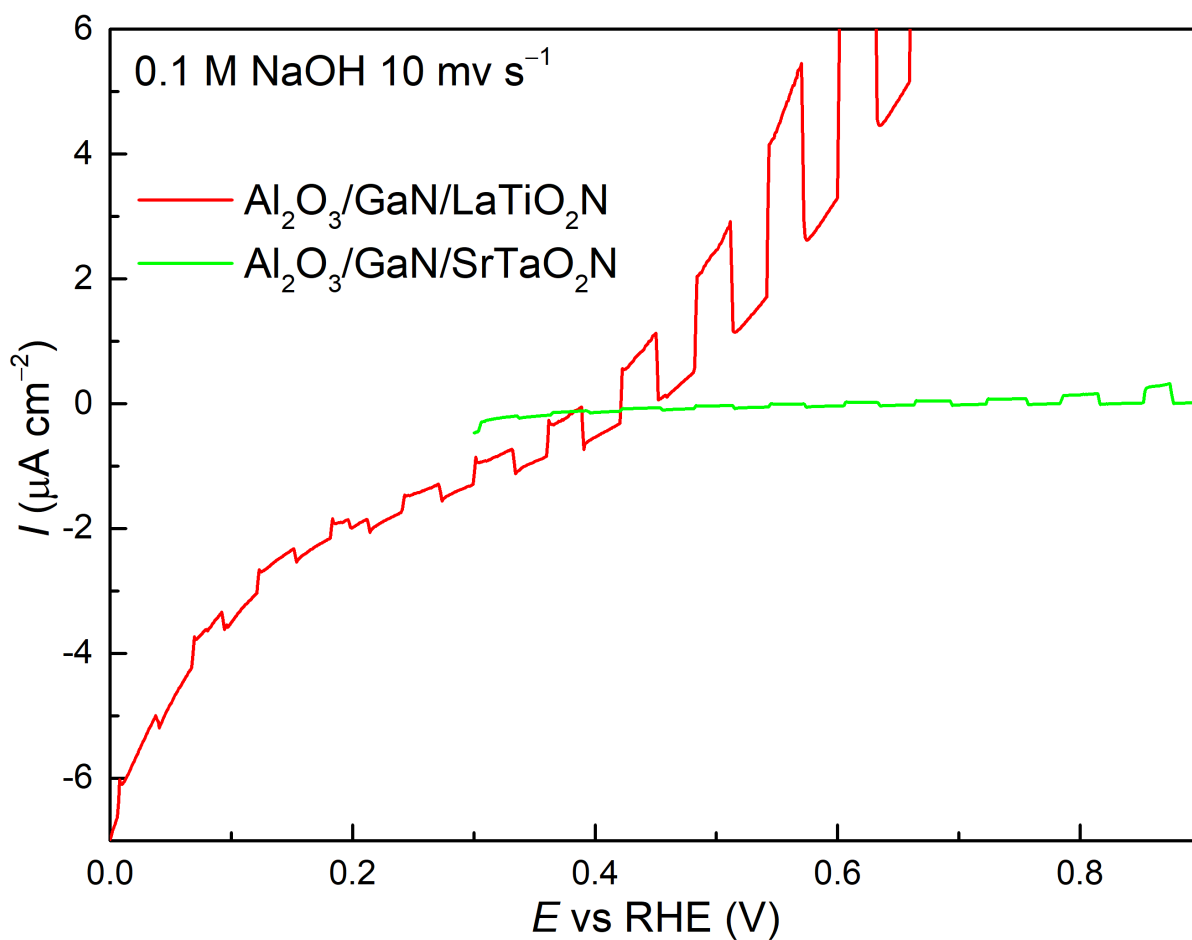


Fig. S9 Enlarged view of the data from Fig. 4d of the main manuscript.

III. References

- 1 A.-D. Li, Y.-J. Wang, S. Huang, J.-B. Cheng, D. Wu and N.-B. Ming, *J. Cryst. Growth*, 2004, **268**, 198–203.
- 2 Z. ZHAO, Y. ZHANG, J. YANG, H. LI, W. SONG and X. ZHAO, *J. Ceram. Soc. Japan*, 2005, **113**, 67–70.
- 3 Z. Shao, S. Saitzek, P. Roussel, A. Ferri, É. Bruyer, A. Sayede, M. Rguiti, O. Mentré and R. Desfeux, *Adv. Eng. Mater.*, 2011, **13**, 961–969.
- 4 M. A. Rodriguez, T. J. Boyle, B. A. Hernandez, D. R. Tallant and K. Vanheusden, *J. Am. Ceram. Soc.*, 2004, **82**, 2101–2105.
- 5 W.-S. Liu, S.-H. Huang, C.-F. Liu, C.-W. Hu, T.-Y. Chen and T.-P. Perng, *Appl. Surf. Sci.*, 2018, **459**, 477–482.